Programme Area: Nuclear

Project: Natural Hazards Phase 3

Title: Volume 10: Space Weather

Abstract:

This technical volume addresses:
• Introduction
• Description of the main phenomena
• Observations and geomagnetic indices
• Methodologies
• Related phenomena; solar energetic particles and ground level enhancement, ionospheric scintillation effects on satellite communication and GNSS signal, GIC and pipelines, hazard combinations
• Regulation
• Conclusion and emerging trends

Context:

The Natural Hazards Review project will develop a framework and best practice approach to characterise natural hazards and seek to improve methodologies where current approaches are inefficient. This is to improve energy system infrastructure design and the project is intended to share knowledge of natural hazards across sectors. The project will be completed in three stages. Phase one will focus on a gap analysis. Phase two will look at developing a series of improved methodologies from the gaps identified in phase one, and phase three will demonstrate how to apply these methodologies. Finally, phase 3 will develop a “how to” guide for use by project engineers.

Enabling Resilient UK Energy Infrastructure: Natural Hazard Characterisation Technical Volumes and Case Studies

Volume 10:

Space Weather

LC 0064_18V10

EDF ENERGY

energy technologies institute

IChemE ADVANCING CHEMICAL ENGINEERING WORLDWIDE

Institution of MECHANICAL ENGINEERS

Met Office

MOTT MACDONALD

Legal Statement

Author: Alexis Ruffenach (EDF Energy)
Chief Technical Officer: Hugo Winter (EDF Energy)

Version	Date	Details
0.1	26/04/18	Submitted for IPR
0.2	04/06/18	IPR comments addressed and submitted to CTO
1.0	12/07/18	CTO comments addressed and submitted to ETI
2.0	08/08/18	ETI and NHP3 Steering Committee comments addressed

Preface

This document forms part of the Energy Technologies Institute (ETI) project 'Low Carbon Electricity Generation Technologies: Review of Natural Hazards', funded by the ETI and led in delivery by the EDF Energy R&D UK Centre. The aim of the project has been to develop a consistent methodology for the characterisation of natural hazards, and to produce a high-quality peer-reviewed set of documents suitable for use across the energy industry to better understand the impact that natural hazards may have on new and existing infrastructure. This work is seen as vital given the drive to build new energy infrastructure and extend the life of current assets against the backdrop of increased exposure to a variety of natural hazards and the potential impact that climate change may have on the magnitude and frequency of these hazards.

The first edition of *Enabling Resilient UK Energy Infrastructure: Natural Hazard Characterisation Technical Volumes and Case Studies* has been funded by the ETI and authored by EDF Energy R&D UK Centre, with the Met Office and Mott MacDonald Limited. The ETI was active from 2007 to 2019, but to make the project outputs available to industry, organisations and individuals, the ETI has provided a licence to the Institution of Mechanical Engineers and Institution of Chemical Engineers to exploit the intellectual property. This enables these organisations to make these documents available and also update them as deemed appropriate.

The technical volumes outline the latest science in the field of natural hazard characterisation and are supported by case studies that illustrate how these approaches can be used to better understand the risks posed to UK infrastructure projects. The documents presented are split into a set of eleven technical volumes and five case studies.

Each technical volume aims to provide an overview of the latest science available to characterise the natural hazard under consideration within the specific volume. This includes a description of the phenomena related to a natural hazard, the data and methodologies that can be used to characterise the hazard, the regulatory context and emerging trends. These documents are aimed at the technical end-user with some prior knowledge of natural hazards and their potential impacts on infrastructure, who wishes to know more about the natural hazards and the methods that lie behind the values that are often quoted in guideline and standards documents. The volumes are not intended to be exhaustive and it is acknowledged that other approaches may be available to characterise a hazard. It has also not been the intention of the project to produce a set of standard engineering 'guidelines' (i.e. a step-by-step 'how to' guide for each hazard) since the specific hazards and levels of interest will vary widely depending on the infrastructure being built and where it is being built. For any energy-related projects affected by natural hazards, it is recommended that additional site- and infrastructure-specific analyses be undertaken by professionals. However, the approaches outlined

aim to provide a summary of methods available for each hazard across the energy industry. General advice on regulation and emerging trends are provided for each hazard as context, but again it is advised that end-users investigate in further detail for the latest developments relating to the hazard, technology, project and site of interest.

The case studies aim to illustrate how the approaches outlined in the technical volumes could be applied at a site to characterise a specific set of natural hazards. These documents are aimed at the less technical end-user who wants an illustration of the factors that need to be accounted for when characterising natural hazards at a site where there is new or existing infrastructure. The case studies have been chosen to illustrate several different locations around the UK with different types of site (e.g. offshore, onshore coastal site, onshore river site, etc.). Each of the natural hazards developed in the volumes has been illustrated for at least one of the case study locations. For the sake of expediency, only a small subset of all hazards has been illustrated at each site. However, it is noted that each case study site would require additional analysis for other natural hazards. Each case study should be seen as illustrative of the methods outlined in the technical volumes and the values derived at any site should not be directly used to provide site-specific values for any type of safety analysis. It is a project recommendation that detailed site-specific analysis should be undertaken by professionals when analysing the safety and operational performance of new or existing infrastructure. The case studies seek only to provide engineers and end-users with a better understanding of this type of analysis.

Whilst the requirements of specific legislation for a sub-sector of energy industry (e.g. nuclear, offshore) will take precedence, as outlined above, a more rounded understanding of hazard characterisation can be achieved by looking at the information provided in the technical volumes and case studies together. For the less technical end-user this may involve starting with a case study and then moving to the technical volume for additional detail, whereas the more technical end-user may jump straight to the volume and then cross-reference with the case study for an illustration of how to apply these methodologies at a specific site. The documents have been designed to fit together in either way and the choice is up to the end-user.

The documents should be referenced in the following way (examples given for a technical volume and case study):

ETI. 2018. *Enabling Resilient UK Energy Infrastructure: Natural Hazard Characterisation Technical Volumes and Case Studies,* Volume 1 — Introduction to the Technical Volumes and Case Studies. IMechE, IChemE.

ETI. 2018. *Enabling Resilient UK Energy Infrastructure: Natural Hazard Characterisation Technical Volumes and Case Studies,* Case Study 1 — Trawsfynydd. IMechE, IChemE.

Contents

1. Introduction

Space weather is defined as a set of processes originating from solar activity that can affect the near-Earth environment. Contrary to solar effects on terrestrial weather which are dominated by the radiation emitted at wavelengths in the visible and infrared parts of the solar spectrum, effects due to space weather are in large part due to contributions from other frequencies of light such as Extreme UV (EUV), X-rays, and gamma (γ) rays, as well as charged particles from the Sun and magnetic fields. A solar storm is characterised by processes (described in *Section 2*) such as:

*Solar wind**

Uninterrupted magnetic and particle flux, called *plasma*, originating from the Sun, whose characteristics (e.g. temperature, density, velocity) vary both during and between different solar cycles.

Solar flares and *coronal mass ejections*

Solar flares are the sudden brightening associated with the solar active regions (sunspots where brief releases of magnetic and thermic energies are observed. During these episodes *solar energetic particles* (SEPs) and magnetised plasma called coronal mass ejections (CMEs are produced. The aforementioned processes impact the *magnetosphere* — the Earth's magnetic shield — in different ways. CMEs are often responsible for generating the most intense geomagnetic storms, which are temporary disturbances of the magnetosphere. The geomagnetic storm may generate geomagnetically induced currents (GICs) in the ground by inductive effects due to the increased electric field propagating into the atmosphere. In this volume, the impacts of extreme geomagnetic storms and associated GICs are discussed in more detail.

These effects have diurnal, seasonal, and solar cycle dependencies. A solar cycle is defined by the peaks and troughs of solar activity, and can be measured, e.g. with sunspot (black spots appearing occasionally on the Sun's surface) number records or solar emissions at EUV or X-ray wavelengths. A solar minimum is defined at minimum activity levels, and a solar maximum conversely is defined at maximum solar activity levels. The average duration from one phase to another (e.g. solar minimum to solar minimum) is 11 years and is referred to as one solar cycle. It is important to highlight that intense space weather events such as flares and coronal mass ejections can be observed throughout the solar cycle, including at the solar minimum.

The largest solar and geomagnetic storm on record was observed by Richard Carrington on 1st September 1859. Carrington observed an abnormally large group of sunspots and subsequent solar flares in his ground-based observatory. This observed solar activity precipitated

*All technical terms marked in blue can be found in the Glossary section.

an abundance of events — a coronal mass ejection, geomagnetic storm, and *aurorae* at low geomagnetic latitudes — whose impacts could be detected at the Earth's surface. This so-called Carrington Event is often selected as a key example of an extreme space weather event.

No storm as powerful as the Carrington Event has occurred since, but society is increasingly more reliant on energy transmission than it was in 1859. Modern society relies upon the grid for needs as diverse as preservation and distribution of food resources, public transportation, and information technology. With increased dependence, the infrastructures supporting the power grid are increasingly more complex and interconnected, making risk assessment, mitigation and prevention more difficult. Additionally, with the modern power grid operating closer to capacity than during the last extreme space weather event, the space weather effects from a future event with a similar intensity to the Carrington Event (a Carrington-type event) are likely to be more widespread than the comparatively minor disruptions experienced in 1859 (e.g. communications disruptions to the telegraph systems). Such events can thus be considered high-impact (or high-consequence) and low-frequency. Recent research in the field of space weather gives a better understanding of how to mitigate, respond to, or even prevent GIC-related damage on a global scale (*NRC, 2008*; *Erinmez et al., 2002*).

Hence, space weather is a scientific discipline which encompasses a broad range of phenomena that impact the terrestrial environment and human-engineered systems in a large variety of ways. In this technical volume, the space weather phenomena that directly and indirectly impact ground-based electrical power grids are the focus of attention; they are briefly described in *Section 2*. In *Section 3*, the observations available to characterise the phenomena are presented and space weather forecast tools are described. *Section 4* deals with the methodology available to define and estimate the intensity of extreme space weather events (geomagnetic storms) in the UK and the steps required to model the GIC associated with these extreme geomagnetic storms. In *Section 5*, other space weather phenomena that might impact ground infrastructure are considered, including the impact of solar energetic particles and increases of neutron irradiation at the ground level. Finally, regulations linked to this hazard are discussed.

It is important to note that, as space weather is a recent research area, the state of the art is evolving at a fast pace. This technical volume is intended to enable the reader to grasp the fundamental aspects and to understand the steps required to characterise the impacts on power network systems. As such, this technical volume does not contain specific estimations of the extreme occurrences for the UK, or detailed GIC estimations, as the current approaches are either not well developed or are open to large uncertainties.

This section focuses on a relatively narrow cross-section of literature on space weather phenomena that directly and indirectly impact ground-based electrical power grids. These phenomena include solar wind, *interplanetary magnetic fields*, CMEs, geomagnetic storms, and GIC, all of which are described briefly. Other phenomena such as SEPs are described in *Section 5*.

2.1 Solar wind and interplanetary magnetic field

The flow of charged particles (ions and free electrons) originating from the Sun is called the solar wind. The gravitational field of the Sun keeps much of the solar atmosphere intact, but particles in the solar corona (outermost part of the Sun's atmosphere) are moving so quickly that some of them escape into interplanetary space in the form of a magnetised plasma-forming solar wind (*Schwenn, 2006*; *Lloyd's 360 Risk Insight, 2011*).

Spacecraft measurements provide evidence of two types of solar wind: a fast solar wind coming from a *coronal hole*, and a slow solar wind from the equatorial region or close to the active region. The slow solar wind has a speed of about 400 kilometres per second (km/s); for the fast solar wind the speed range is 700 to 800 km/s. The high-speed solar wind streams interact with the low-speed streams to produce regions of enhanced magnetic field strength and particle density, called *coronal interaction regions (CIR)* (*Schwenn, 2006*; *Denton et al., 2006*). These may be associated with geomagnetic storms of low intensity.

The interplanetary magnetic field (IMF), which starts at the Sun, is embedded in the solar wind. The IMF magnitude varies with the solar cycle. At distances of one *astronomical unit* (au, the distance between the Sun and the Earth), the IMF strength varies between about 6 and 9 *nanotesla* (nT). The orientation of the solar wind magnetic field (magnetic field vector B) is important in the context of magnetic storm occurrence, particularly the value of the z-component B_z (the z-axis is defined as parallel to the Earth's magnetic dipole axis). A positive B_z can compress the magnetosphere and cause an electromagnetic disturbance at the surface of the Earth (*Dungey, 1961*). However, the parallel field is mostly repelled by the magnetospheric field, and the repercussions are minor compared to those from an antiparallel, south-pointing B_z (*MITRE, 2011*). These southward fields cause geomagnetic storms and are typically associated with CMEs.

2.2 Coronal mass ejections

While the solar wind outflow can be considered as steady mass loss from the Sun, CMEs are more intense and their generation is scattered. A CME consists of plasma (primarily electrons

and protons) which can be described in terms of its density, temperature, and bulk speed. The CME and solar wind also carry an embedded magnetic field. When the CME reaches the vicinity of the Earth, it interacts with the magnetosphere: the topology of the magnetic field lines is modified which enables a transfer of the energy into the magnetosphere. Usually, there are a few CMEs per day (*Aschwanden, 2005*). More than 20,000 CMEs have been detected by the Solar and Heliospheric Observatory (SOHO satellite) between 1996 and 2013, a period covering more than one solar cycle (*Yashiro et al., 2004*). For ground-level effects, the most relevant CMEs are those that travel radially toward Earth, deemed *halo* or Earth-directed CMEs that probably originated on the western limb of the Sun and followed the *Parker spiral* of the IMF (*Aschwanden, 2005*).

The ability of a CME to generate geomagnetic storms is related to two parameters: its radial velocity and the vertical component (B_z) of its magnetic field (intensity and orientation southward or northward). Faster CMEs produce more severe effects (*Gosling et al., 1990*), and it appears that intense solar storms are associated with CMEs, whereas the medium or low intensity storms are more associated with fast solar winds and CIR (*Richardson and Cane, 2013*). As an example of extreme CME speeds, *Cliver et al. (2013)* estimated that the CME related to the 1859 Carrington Event took ~17.6 hours (h) to travel the distance from the Sun to the Earth, suggesting an average speed of ~2400 km/s (*Riley, 2012*). For the magnitude of B_z, *Siscoe et al. (2006)* and *Temerin and Li (2006)* model the Carrington-type event using an intensity of the magnetic field equal to 132 nT and 60 nT respectively.

During periods of high solar activity, the Sun can launch several CMEs towards the Earth and these may collide during their transit to the Earth. This can disturb the plasma sheet at the boundary between CMEs, which can increase the magnitude and the orientation of the magnetic field contained within it.

2.3 Geomagnetic storms

A southward B_z component of the IMF can lead to *magnetic reconnection* of field lines that occur on the *dayside*. In the reconnection process, the oppositely-aligned IMF and geomagnetic field lines combine and move with the solar wind away from the Sun into the magnetospheric tail (*magnetotail*). The flux transfer then drives the convection of plasma back toward the Earth. Additionally, the solar wind velocity and z-component of the magnetic field contribute to the convective electric field that points from dawn to dusk (*Goldstein, 2006*; *MITRE, 2011*). *Figure 1* is a representation of the magnetic reconnection process, which is defined by the coupling of the solar wind and the magnetosphere that occurs during the crossing of a CME (or

solar wind) whose magnetic field may be oriented southward. The magnetospheric response is associated with a topological modification of the magnetic field dayside due to the magnetic reconnection process. The magnetic reconnection process allows solar wind energy to enter the magnetosphere, where it is transported to the nightside of the Earth and temporarily stored in the tail of the magnetosphere. When the stored energy reaches some critical level, it is released explosively, and some of that energy is directed towards Earth and into the ionosphere at higher latitudes, generating geomagnetic disturbances. These geomagnetic disturbances (GMDs, changes in the magnetic field with respect to time) induce geoelectric fields and currents when the GMDs propagate to the ground level (*MITRE, 2011*; *Pulkkinen et al., 2012*). Aurorae are generated during these processes (as modelled in *Figure 2*).

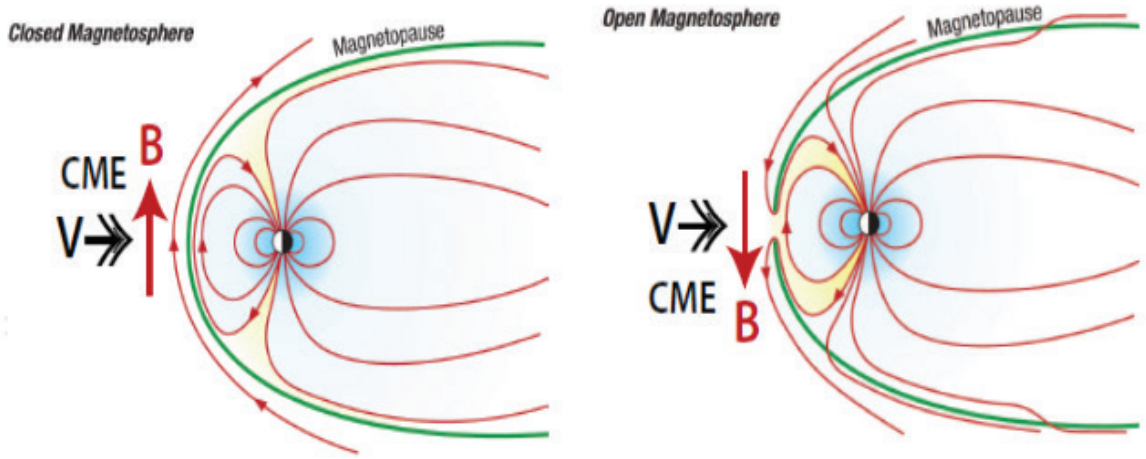

Figure 1. Schematic of a CME impacting the magnetosphere. In the left panel, the magnetic field contained in the CME is parallel to the magnetosphere and thus compresses it. In the right panel, the anti-parallel CME magnetic fields reconnect with the magnetosphere. Adapted from J. A. Eddy, The Sun, the Earth, and Near-Earth Space: A Guide for the Sun-Earth System *(Eddy, 2009).*

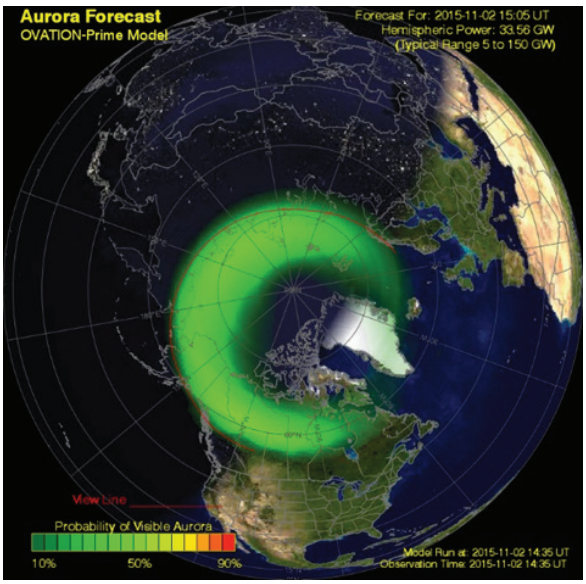

Figure 2. Visibility of the northern aurora oval on November 2, 2015, from the OVATION Aurora Forecast Model (SWPC, 2018a).

2.4 Geomagnetically induced current

Electric fields are generated in the ground during severe space weather events due to the induction effects of a changing magnetic field near the surface. During large geomagnetic storms, GICs associated with electric fields can flow through the ground as illustrated by *Figure 3*. The geomagnetic latitude of the UK is similar to its geographic latitude — approximately 50 to 60° North — placing it in a region of similar risk level as southern Canada and the northern United States. This latitude is near the peak of the *auroral electrojet* (a large horizontal current flowing in the ionosphere) during moderate to large disturbances, which are the primary drivers of GICs. GICs can cover a large geographic area, but the specific impact from any given storm is likely to be more localised due to small-scale local conductivity structure. Certain areas are thus more prone to significant impacts during any geomagnetic storm, and this depends on the geomagnetic latitude, proximity to the auroral electrojet, and specific conductivity profiles. In the UK, typical ground-level electric field strengths are of the order of 0.1 volts per kilometre (V/km) during periods of quiet space weather, but may rise to ~5 to 10 V/km during severe space weather events (e.g. during the October 2003 storm) (*Thomson et al., 2005*). This means that the potential difference across the ends of a conductor of length 100 km would be 0.5 to 1 kilovolts (kV). As such, high voltage power systems can be vulnerable to GICs, particularly where they offer a low-resistance path for the current compared to the ground (*Beggan et al., 2013*; *Beggan, 2015*).

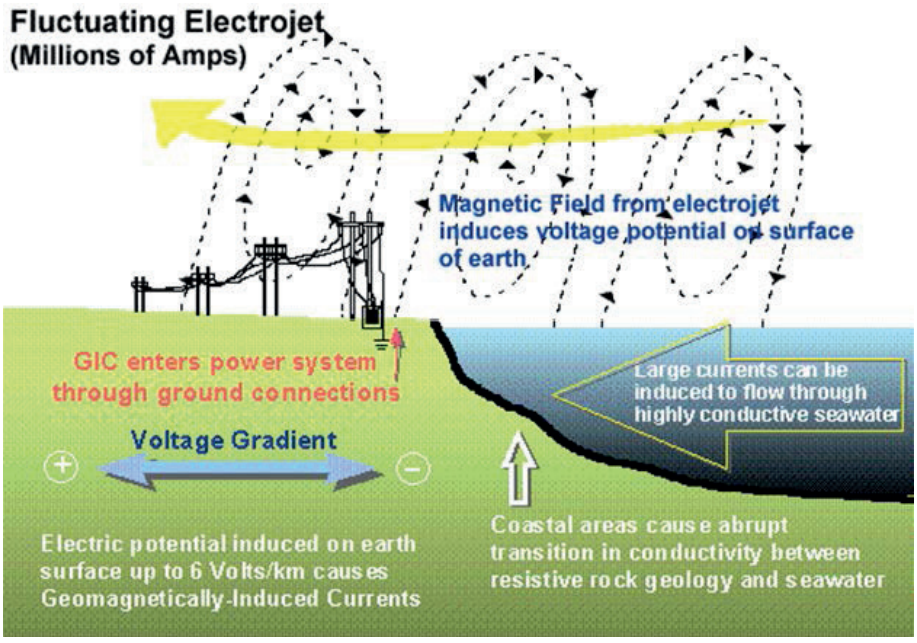

Figure 3. Illustration of auroral electrojet influence on the electricity network. Intense geomagnetic storms can create large electrojet currents in the atmosphere leading to GIC generation in the ground due to inductive effect. Near the coasts, electric field enhancements can occur due to lateral variations in conductivity. (© Metatech Corporation)

2.5 Chronology of a solar storm

One of the challenges in defining an extreme space weather scenario for the UK power network is that no two solar storms are alike (*Lanzerotti, 1992*). For this reason, it is instructive to describe the characteristics of a typical solar storm, while acknowledging that each individual event can differ considerably. Based on an analysis of several events, the Royal Academy of Engineering report (*RAE, 2013*) outlined the general chronology of a solar storm, as follows:

- The storm starts with the development of one or more complex sunspot groups which are seen to track across the solar surface.
- From within these active regions, one or more solar flares are produced and are then detected on Earth only eight minutes later. Many of these will be A-, B- and C-class flares, but a few will be M- and X-class. This classification of electromagnetic flux near the Earth is based on peak flux measured by a GOES spacecraft (from A to X, defined as the least to the most energetic respectively).
- Highly energetic (relativistic) solar particles are released and detected just a few minutes later both by satellites and at ground level. These continue to arrive over a period of hours, and even days if further eruptions occur.

A CME occurs and travels at many hundreds of km/s, taking ~15 to 72 h to arrive at the orbital distance of the Earth. The level of impact on Earth is dependent on the speed of the CME, how close it passes with respect to Earth, and the orientation of the magnetic fields in the CME and in the compressed solar wind ahead of the CME. For example, a CME travelling faster than 800 km/s can generate shocks in the solar wind, thereby accelerating charged particles. In addition, a southward component of the magnetic field allows the CME to interact strongly with the magnetosphere, becoming *geo-effective* (see also *Section 2.3*)

2.6 Summary: key phenomena

A solar storm encompasses three main components (*Marusek, 2007*) — solar flares, SEPs and CMEs. The main physical properties of these phenomena are summarised in *Table 1*, and the three events are visualised in *Figure 4*. The physical processes related to the generation of GIC have been emphasised; this included the generation and propagation of CMEs and the geo-magnetic storms. *Section 5* provides more information on SEPs and their associated impacts.

Table 1. Summary of key space weather phenomena (Marusek, 2007; Launay, 2014).

	Solar flares	Solar energetic particles (SEPs)	Coronal mass ejections (CMEs)
Physical nature	X-rays, extreme UV, gamma rays	Energetic protons and ions (typically 10 to 100 MeV, but up to 20 GeV)	Vast plasma clouds containing relatively low to medium energy particles with embedded magnetic field
Time needed to reach Earth	8 minutes (speed of light)	15 minutes to 24 hours	1 to 4 days
Duration of interaction with Earth	Minutes to hours	Several days	1 to 2 days

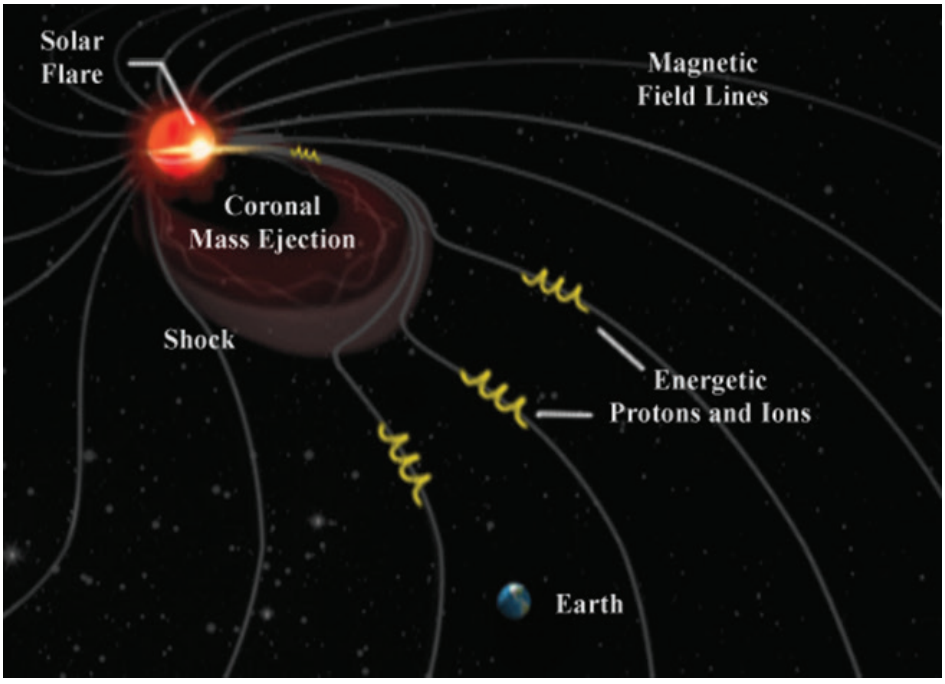

Figure 4. Illustration of solar flares, SEPs and CME, showing the protons being guided by, and gyrating around, the IMF. The IMF forms a roughly spiral pattern due to the rotation of the Sun (UMA, 2018).

This section describes observations used by space weather forecast centres. Space weather forecast centres monitor, analyse and forecast space weather. They provide information to different sectors such as aeronautics and space industries, power utilities, geophysicists and the military. Geomagnetic indices, which indicate the severity of the geomagnetic disturbances, are also presented.

3.1 Observations available

There are many data sources associated with the space weather field which are provided by instruments either in space — on board satellites and spacecraft — or at ground level. Most of the data are freely available through governmental institutes such as the National Aeronautics and Space Administration (NASA) (Coordinated Data Analysis Web) or European Space Agency (ESA) (Space Situational Awareness — Solar Weather) (*NASA, 2018*; *ESA, 2018*). The interpretation and analysis of these data is not straightforward for the non-specialist. To facilitate the dissemination of information and alert the public in case of forthcoming events, space weather forecast centres have been created in recent years; there are several across the world (e.g. US, UK, Canada, Australia).

Models used by space weather forecast centres are developed to provide, with reasonable warning time, predictions of the interplanetary environment. Due to the complexity of the processes involved between the Sun and the Earth, various models must be coupled. Space weather centres have been created to collect real time data and implement prediction models. In the UK, a forecast centre was recently created in Exeter (Met Office Space Weather Operations Centre — MOSWOC, *Figure 5a*) and is managed by the Met Office.

Figure 5b presents an example of the different space products and processes analysed during a solar eruption. For an extreme geomagnetic storm such as a Carrington-type event, the potential timeline should be:

- 15 to 18 hours before the storm, the perturbed solar atmosphere (presence of coronal hole, sunspots and filaments) should be observed by solar imagery. An extremely rapid CME will be produced, associated potentially with a flare of class X.
- A solar wind propagation model (ENLIL: physics-based prediction model of the heliosphere) permits the calculation of the arrival time of the CME on Earth.
- 15 to 30 minutes before the storm, the CME's characteristics — such as the intensity and orientation of its magnetic field — are known thanks to spacecraft such as the Advanced Composition Explorer (ACE).
- When the storm commences, the CME reaches the Earth and generates a geomagnetic storm. The rate of change of the magnetic field will vary for several days. These variations are measured by a network of magnetometers located across the Earth.

(a)

(b)

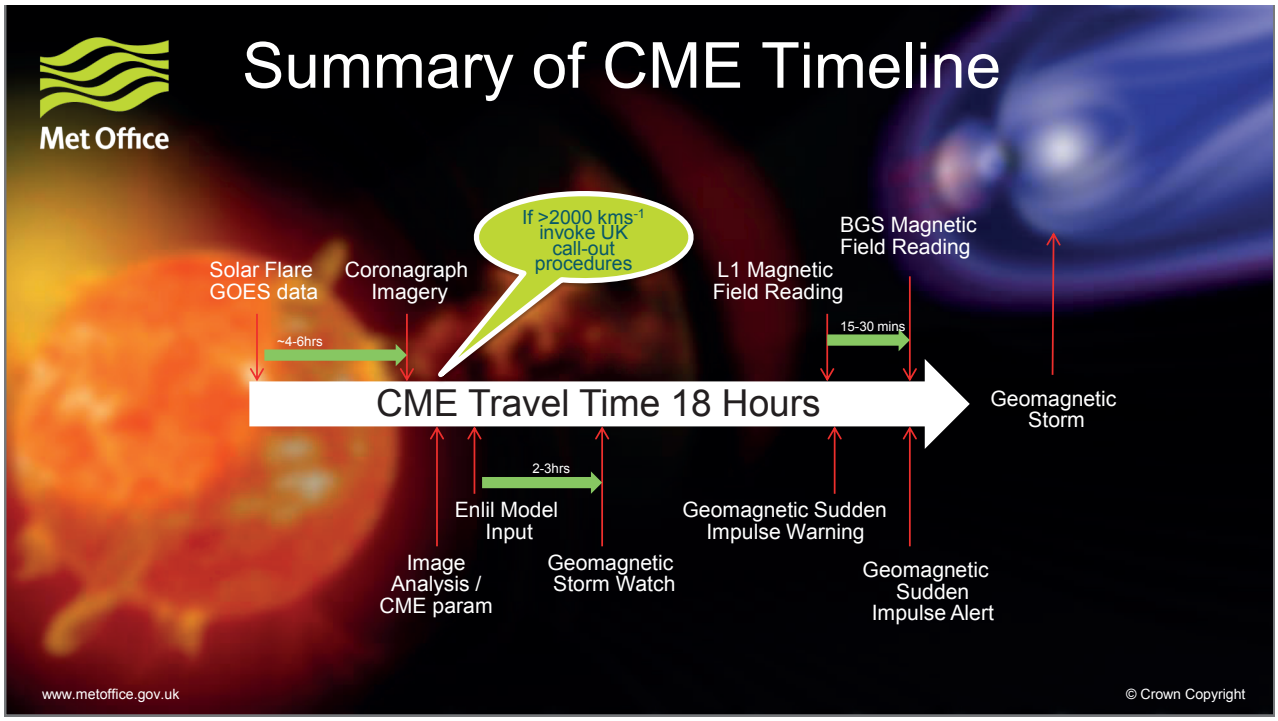

Figure 5. (a) Photograph of the Met Office's Space Weather Operations Centre in Exeter.
(b) Chronology of the observations and forecast of CME during its propagation from the Sun to Earth. The different products delivered are mentioned (measurement of solar flux GOES data, solar imagery observations, in situ CME measurement with ACE spacecraft such as magnetic field reading, and terrestrial magnetic field variation with British Geological Survey (BGS) reading). Analysis is undertaken to characterise the interplanetary medium through simulations of solar wind parameters with ENLIL model. In the case of CME with an average speed of 2000 km/sec (corresponding to a 18 hour time travel of the CME to the Earth) or greater, the Met Office may initiate a procedure to alert stakeholders of a potential risk for their assets. (© Crown Copyright Met Office 2018)

3.2 Geomagnetic indices

The intensity of geomagnetic storms can be analysed though the variations of geomagnetic indices. The K_p index is a quasi-logarithmic scale derived from binned local magnetic activity observations (from a network of geomagnetic observatories) that have been scaled to local average conditions. This scale uses an integer in the range 0 to 9 to quantify disturbances in the horizontal component of the magnetic field of the Earth. A K_p value of 1 indicates calm conditions, while a value of 5 or more indicates a geomagnetic storm.

The disturbance storm time and auroral electrojet indices (*Dst* and *AE*, respectively) are other global indices that are sometimes used in GIC hazard analysis. The *Dst* index gives information about the strength of the *ring current* in the lower magnetosphere, which is the main physical cause for the ground magnetic perturbations at low latitudes. The ring current is composed of ions and electrons and flows westward around the Earth in the equatorial plane at an altitude of several Earth radii (~15 to 30 x 10^3 km).

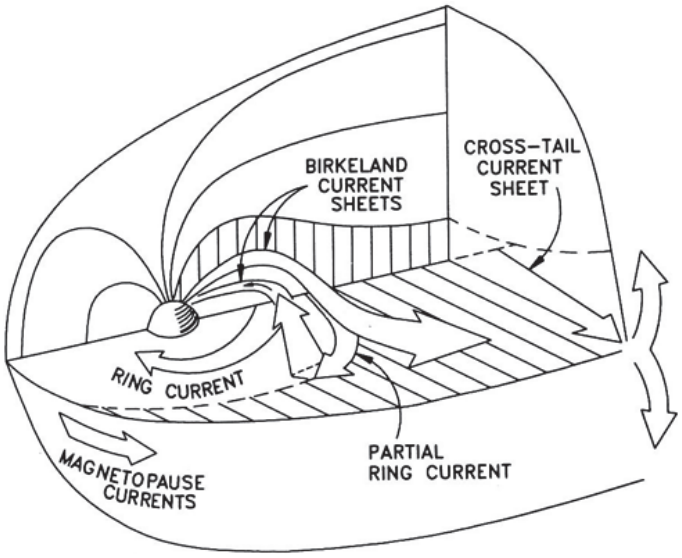

Figure 6. Illustration of the Earth current system (Stern, 1994). In this figure, the Sun is located far to the left of the Earth.

The magnetic field produced by the ring current is directly opposite to the magnetic field of the Earth. An illustration of the Earth current system is provided in *Figure 6*. During magnetic storms, the ring current receives additional ions and electrons from the night-side magnetotail, and its effect increases. To quantify this effect, a negative *Dst* value indicates a diminished geomagnetic field strength (*Baumjohann and Treumann, 2004*). The well-known geomagnetic storm during the Quebec event of 13th to 14th March 1989 was the largest of the modern era, with *Dst* falling to –589 nT (*Li et al., 2006*). For comparison, the estimates of *Dst* for the Carrington-type event range from –1760 nT to –850 nT (*Tsurutani et al., 2003*; *Siscoe et*

al., 2006). In the absence of more locally-specific information, *Baker et al. (2013)* note that negative *Dst* values of less than −300 nT signal to the space weather user community that a powerful geomagnetic storm is under way.

The *Dst* index is useful because it is commonly used as a descriptor of the intensity of the main phase of magnetic storms (*Sugiura and Kamei, 1991*). An ideal geomagnetic storm is identified by three phases: an initial phase, a main phase, and a recovery phase. The main phase is characterised by a *Dst* index lower than −50 nT. The time duration of the main phase is between 2 and 8 hours. The recovery phase may last between 8 hours and 7 days during which the magnetic field intensity returns to normal level. However, the *Dst* index is derived solely from low-latitude magnetic observatories, making it less useful for mid- to high-latitude local analysis. The absolute deviation in the field (as is used to classify magnetic storms) has less GIC relevance than the rate of change of the field and the spectral composition of the magnetic field time series. This information is provided by magnetometers; there are three magnetometers in the UK, located at Lerwick, Eskdalemuir and Hartland.

3.3 Geomagnetic storm scale

To quantify the impact of geomagnetic storms driven by CMEs, MOSWOC uses the G-scale which is closely associated with the index K_p. More information about the impacts corresponding to each G or K_p level are provided in *Table 2*. The value of the G scale equals $K_p - 5$, meaning that a minor storm (G1) corresponds to $K_p = 5$, while an extreme storm (G5) corresponds to $K_p \geq 9$.

G5 events typically occur in the order of four per 11-year solar cycle. While it seems plausible that the Carrington-type event would have been classified as extreme (G5 or more: G5+), recent major storms have tended to be severe rather than extreme. For instance, the geomagnetic disturbances on 29th to 30th October 2003 (*Kappenman, 2005*) and 15th July 2000 (*Tripathi and Mishra, 2006*) are both classified as G4 events. However, the March 1989 event, which caused the collapse of the Hydro-Quebec network, appears to be classified as G4 to 5 (*Allen et al., 1989*). It should be noted that similar scales exist for radiation storms and radio blackout (*Met Office, 2015*).

Table 2. G-scale for geomagnetic disturbances (Met Office, 2015). Adapted by the Met Office, from NOAA Space Weather Scales, to include UK effects.

Category		UK effect	US and global effect	Physical measure	Average frequency (1 cycle = 11 years)
Scale	Descriptor	Duration of event will influence severity of effects			
		Geomagnetic storms		K_p values*	Number of storm events when K_p level was met: (number of storm days)
G5	Extreme	**Power systems**: localised voltage control and protective system problems may occur leading to potential for localised loss of power. Transformers may experience damage.	**Power systems**: widespread voltage control problems and protective system problems can occur, some grid systems may experience complete collapse or blackouts. Transformers may experience damage.	$K_p = 9$	4 per cycle (4 days per cycle)
		Spacecraft operations: may experience extensive surface charging, drag may increase on low-Earth-orbit satellites, problems with orientation and uplink/downlink and tracking satellites.	**Spacecraft operations**: may experience extensive surface charging, problems with orientation and uplink/downlink and tracking satellites.		
		Other systems: HF (high-frequency) radio communication may be impossible in many areas for one to two days, GNSS (GPS) satellite navigation may be degraded for days with possible effects on infrastructure reliant on GNSS (GPS) for positioning or timing, low-frequency radio navigation can be out for hours, and aurora may be seen across the whole of the UK.	**Other systems**: pipeline currents can reach hundreds of amps, HF (high-frequency) radio communication may be impossible in many areas for one to two days, satellite navigation may be degraded for days, low-frequency radio navigation can be out for hours, and aurora has been seen as low as Florida and Southern Texas (typically 40° geomagnetic lat.)**.		
G4	Severe	**Power systems**: no significant impact on the UK power grid likely.	**Power systems**: possible widespread voltage control problems and some protective systems will mistakenly trip out key assets from the grid.	$K_p = 8$, including a 9–	100 per cycle (60 days per cycle)
		Spacecraft operations: may experience surface charging and tracking problems, drag may increase on low-Earth-orbit satellites, corrections may be needed for orientation problems.	**Spacecraft operations**: may experience surface charging and tracking problems, corrections may be needed for orientation problems.		
		Other systems: HF radio propagation sporadic, GNSS (GPS) satellite navigation degraded for hours, low-frequency radio navigation disrupted, and aurora may be seen across the whole of the UK.	**Other systems**: induced pipeline currents affect preventative measures, HF radio propagation sporadic, satellite navigation degraded for hours, low-frequency radio navigation disrupted, and aurora has been seen as low as Alabama and northern California (typically 45° geomagnetic lat.)**.		
G3	Strong	**Power systems**: no significant impact on the UK power grid likely.	**Power systems**: voltage corrections may be required, false alarms triggered on some protection devices.	$K_p = 7$	200 per cycle (130 days per cycle)
		Spacecraft operations: surface charging may occur on satellite components, drag may increase on low-Earth-orbit satellites and corrections may be needed for orientation problems.	**Spacecraft operations**: surface charging may occur on satellite components, drag may increase on low-Earth-orbit satellites and corrections may be needed for orientation problems.		
		Other systems: intermittent GNSS (GPS) satellite navigation and low-frequency radio navigation problems may occur, HF radio may be intermittent. Aurora may be seen in Scotland and Northern Ireland, and as low as Mid-Wales and the Midlands.	**Other systems**: intermittent satellite navigation and low-frequency radio navigation problems may occur, HF radio may be intermittent, and aurora has been seen as low as Illinois and Oregon (typically 50° geomagnetic lat.)**.		
G2	Moderate	**Power systems**: no impact on the UK power grid.	**Power systems**: high-latitude power systems may experience voltage alarms, long-duration storms may cause transformer damage.	$K_p = 6$	600 per cycle (360 days per cycle)
		Spacecraft operations: corrective actions to orientation may be required by ground control; possible changes in drag affect orbit predictions.	**Spacecraft operations**: corrective actions to orientation may be required by ground control; possible changes in drag affect orbit predictions.		
		Other systems: HF radio propagation can fade at higher latitudes, and aurora may be seen across Scotland.	**Other systems**: HF radio propagation can fade at higher latitudes, and aurora has been seen as low as New York and Idaho (typically 55° geomagnetic lat.)**.		
G1	Minor	**Power systems**: no impact on the UK power grid.	**Power systems**: weak power grid fluctuations can occur.	$K_p = 5$	1700 per cycle (900 days per cycle)
		Spacecraft operations: minor impact on satellite operations possible.	**Spacecraft operations**: minor impact on satellite operations possible.		
		Other systems: aurora may be seen as low as Northern Scotland.	**Other systems**: migratory animals are affected at this and higher levels; aurora is commonly visible at high latitudes (northern Michigan and Maine)**.		

**The K_p-index used to generate these messages is derived from a real-time network of observatories that report data to SWPC in near real-time. In most cases the real-time estimate of the K_p-index will be a good approximation to the official K_p-indices that are issued twice per month by the German GeoForschungsZentrum (GFZ) [Research Center of Geosciences].*

*** For specific locations around the globe, use geomagnetic latitude to determine likely sightings (Tips on Viewing the Aurora).*

3.4 GIC scenarios based on geoindices

There are no GIC-specific space weather indices or real-time indicators in common use for GIC hazard assessment. In the US, the National Oceanic and Atmospheric Administration (NOAA) Space Weather Prediction Centre (SWPC) provides forecast alerts of the global K_p index (*SWPC, 2018b*). Although this index can provide a rough indicator of magnetic activity, which is the driver of the GIC hazard, its global nature and formulation from purely magnetic measurements does not provide any local context. In addition, the wide range of magnetic activity specified by the highest K_p designation (K_p = 9) makes it less than useful for GIC specification in a practical setting. As a part of US federal operations requirements (FERC EOP-010-1), these indices are used by the operational centres for the bulk power system to provide an alert of potential geomagnetic disturbances.

3.5 Summary: observation and geomagnetic indices

Space weather forecast centres deliver essential information to characterise the solar and close extra-terrestrial environment. Alerts will be sent including the likelihood of the intensity impact as detailed in *Table 2*. The local level response can be confirmed when the polarity of the CME is known (elapsed time <60 min before effects on Earth). There is currently no specific real-time indicator for GIC assessment. The main driver of GIC is the rate of change of the magnetic field measured by a network of magnetometers on Earth.

This technical volume deals with space weather hazards with the main focus on the impacts of geomagnetic storms on electric transmission systems. Assessing this risk is difficult since, as highlighted in previous sections, space weather is a multi-variable and large-scale phenomenon. Also, the factors that control GICs and the local variations of the associated processes at ground level are still poorly understood (*Schrijver et al., 2015*).

Different levels of assessment may be carried out at spatial scales ranging from global to local. They all require the evaluation of the intensity of GIC and their impacts on electric transmission systems. A brief summary of the different types of analysis required at each spatial scale is provided below:

Global scale

Definition of geomagnetic storm scenarios and their likelihood of occurrence. Firstly, the geomagnetic storm scenario has to be selected, i.e. the intensity (may be based on geomagnetic indices) and location of the storm (electrojet current). A Carrington-type event is commonly considered as an example of an extreme geomagnetic storm.

Regional scale

Estimation of the surface geoelectric field and GIC at the substation level. The variation in the rate of change of the ground-level magnetic field over time alters at different latitudes. Geomagnetic field records and ground conductivity maps are required information to calculate the surface geoelectric field. The geoelectric field (V/km) can be considered as a preliminary risk indicator for the electric transmission network or pipeline (*Section 5.3*). Then, GIC impacts need to be simulated throughout the network using the electric transmission network characteristics.

Local scale

Assessment of system response. *Saturation* of specific transformers and the *reactive power* loss can be estimated.

The structure of this section follows the structure outlined above, from global to local. Firstly, the likelihood of extreme geomagnetic storms occurring in the UK is discussed. Then, the different elements required to simulate GIC are outlined. Finally, past GIC analyses for the UK network and the impact expected on transformer systems are summarised.

4.1 Estimation of the annual probability of exceedance of extreme geomagnetic storms

Based on the intensity of the geomagnetic indices assumed for a Carrington-type event and its related magnetic field intensity at ground level across the UK, it is possible to estimate the annual occurrence probability of an extreme geomagnetic storm along with the intensity of the potential associated GICs. However, given the limited information on the Carrington-type event, and sparse experience of other extreme space weather events, it is difficult to estimate the return period of such events. *Riley (2012)* described one such calculation, suggesting a 12% chance of having a Carrington-type event in the next decade and, therefore, a return period of ~80 years. However, this value was based on disputable statistical analyses and probably overestimates the likelihood of a Carrington-type event. Other estimates for the recurrence rate of a Carrington-type event range from ~100 years (*BEIS, 2015*) and ~150 years (*Lloyd's, 2013*) to >1000 years (*Tsubouchi and Omura, 2007*) depending on the assumed *Dst* value of the event and the statistical method chosen.

Previous studies have used geomagnetic indices as opposed to local parameters. The key quantity in determining the local magnitude of a GIC is the rate of change of the ground-level magnetic field over time; more specifically, its component in the horizontal plane, $\frac{dB_h}{dt}$ (*Viljanen et al., 2001*). It is, therefore, important to assess the plausible extreme values of $\frac{dB_h}{dt}$ over the UK, and the factors which can lead to such values (e.g. the position of the auroral electrojet).

Thomson et al. (2011) performed an extreme value analysis of B_h observations at different geomagnetic latitudes in Europe to understand how extreme geomagnetic storms can be. Both the measured and extrapolated extreme values were found to generally increase with geomagnetic latitude. However, there is a marked maximum between 53° and 62° North. *Thomson et al. (2011)* attribute this to an enhanced auroral electrojet, which tends to move southwards under strong forcing from the solar wind. Since the UK is within this region of enhanced magnetic field activity, it can experience the associated impacts during major geomagnetic storms.

Based on their analysis of the observations, *Thomson et al. (2011)* estimated return levels of extreme space weather events. For example, for a 1-in-100 year event (i.e. an annual exceedance probability, AEP, of 0.01), the horizontal field changes at typical mid-latitude European observatories (55 to 60° geomagnetic latitude) are 1000 to 4000 (nanotesla/minute) nT/min, while compass variations are ~3 to 8° per minute. For a 1-in-200 year event (i.e. an AEP of 0.05) the equivalent values are 1000 to 6000 nT/min and 4 to 11° per minute. For comparison, in an assessment predicting extreme GICs in the UK high-voltage power network, *Beggan et al. (2013)* employed a maximum $\frac{dB_h}{dt}$ = 5000 nT/min. However, it is important to bear in mind that these values are based on statistical analyses of the available data, and do not impose or imply any physical constraints. It is therefore useful to compare them to the largest measured value in the UK, 1100 nT/min (recorded in 1991).

Future studies should continue to investigate the probability of extreme events both by using updated global parameters (geomagnetic indices, CME parameters) and regional parameters (value of the magnetic field rate of change).

4.2 Geomagnetically induced current: key elements

The simulation of GICs requires knowledge of the magnetic field driver of the storm, the deep Earth conductivity that converts a magnetic field driver into an induced surface electric field, and knowledge of the UK power grid and system assets. The magnetic field time series specific to the UK for a Carrington-type event are required to simulate extreme events. The different technical elements required to simulate such an event are presented here. The complete description of the methodology is beyond the scope of this technical volume. The reader should refer to the literature (for instance *Boteler, 2014*).

4.2.1 Conductivity model

The conductivity structure of the UK has been modelled extensively in the European Risk for Geomagnetically Induced Currents project (EURISGIC, European Union FP7 project) (*Ádám et al., 2012; Viljanen et al., 2012; Viljanen et al., 2014*). *Figure 7* shows an example of the conductivity model provided by the EURISGIC project. The conductivity model implemented consists of a 1D model characterised by several different conductivity blocks. The numbering of the blocks follows the convention of EURISGIC and is split according to the geological terrain in UK. Only the upper 3 km layer is represented.

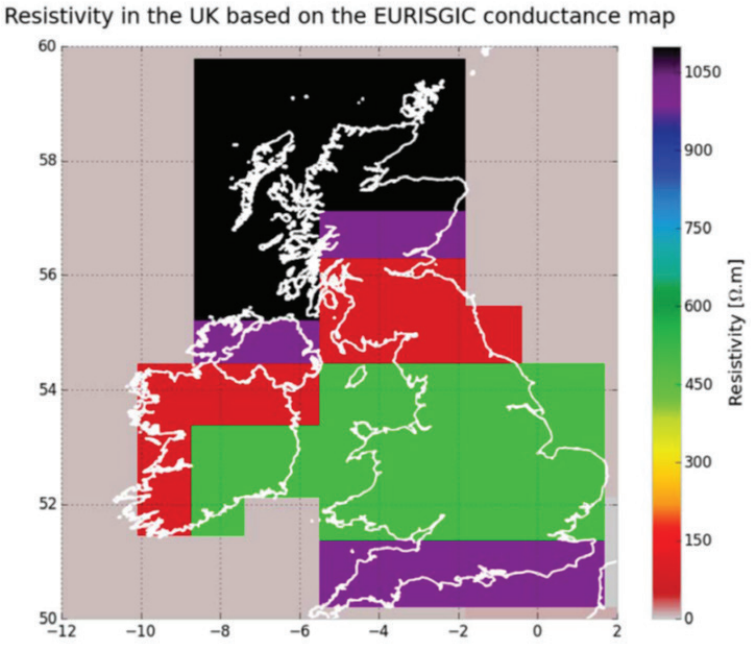

Figure 7. Ground block resistivity map of the UK based on the FP7 European Project EURISGIC. The colour scale indicates the surface layer resistivity. (Viljanen, 2012). Numeric values detailed can be found in REAL (2012).

While the magnetic field is the driver of GIC, deep Earth conductivity determines the magnitude of the induced electric field response that the Earth will produce. A complete analysis of electric field induction would require a detailed 3-D conductivity model of the UK. The EURISGIC models used in this example are simplified and are intended to provide a first-order estimate. As such, they do not include 3-D structure, an omission which can lead to electric field reductions along resistivity model boundaries. In addition, the EURISGIC models are not very well resolved at shallow depths. This means that electric field induction due to the higher frequency magnetic field fluctuations could be underestimated.

A conductive layer tends to reduce the intensity of regional GIC in geophysical terms. For example, lower levels of geoelectric field are generally observed at locations characterised by sedimentary ground, compared to non-conductive igneous volcanic regions (see *Section 4.2.2*). However, a local scale conductive layer could reduce the transformer's earthing resistance, thus increasing its susceptibility to GIC.

4.2.2 Surface electric field model

The interaction of the external magnetic field with the Earth's surface can be approximated by thin-sheet modelling (*Vasseur and Weidelt, 1977*); this determines the electric field arising at a specific single (time) frequency from the layers of conductive material in the sub-surface. The surface electric field varies depending on the interaction of the external magnetic field with the

ground conductivity. The external magnetic field is the driving source term for the induced currents. It is derived through the application of the Spherical Elementary Current System technique (*Amm, 1997*) to data from nearby observatories. *Figure 8* illustrates a surface electric map for an intense geomagnetic storm that occurred in October 2003 (known as the Halloween event); the variation of the electric field intensity across the UK gives a first-order risk assessment.

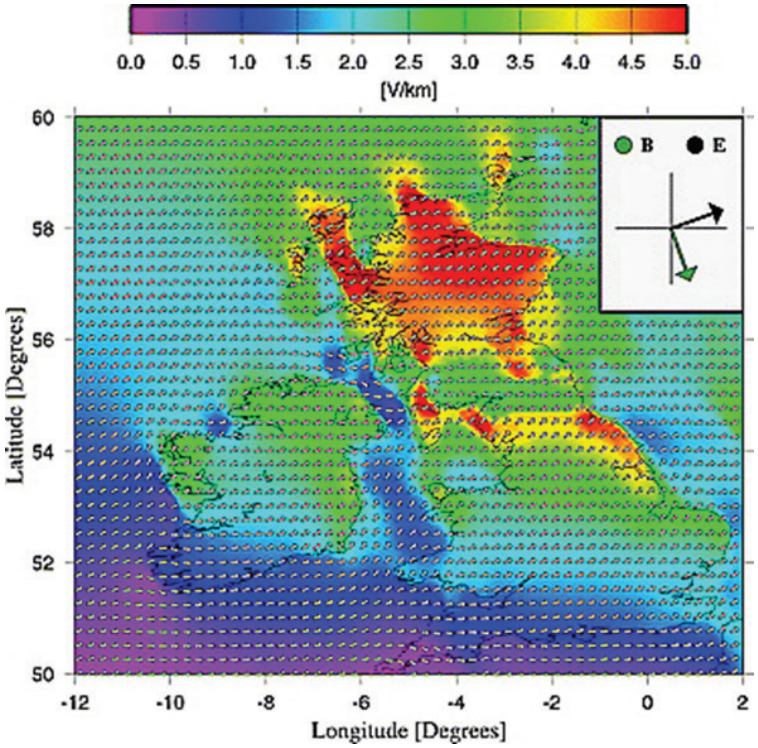

Figure 8. Surface electric field at 2120 UTC on 30 October 2003. Colour denotes e field amplitude (see scale bar) in V/km. Small arrows denote the local field direction (Thomson et al., 2005).

4.2.3 Power network model

The power transmission network in the UK is a high-voltage (HV) system at 400 kV and 275 kV and is owned by the National Grid Company (NGC). It contains 323 substations with 98 transformers connecting the 400 kV systems to the 275 kV systems and 567 transformers connecting the 400 kV and 275 kV systems to the 132 kV systems that provide customers with electricity (*Erinmez et al., 2002*). It is important to highlight that the network configuration is not static. Most of the substations contain more than one transformer for redundancy. The substations without backups are in remote regions where a smaller population will be affected by a failure (*RAE, 2013*). The network is linked to others (e.g. in France, Holland and Northern Ireland) via underwater direct current (DC) connectors which are not affected directly by GICs, though the alternating current (AC)-DC converters may be affected by additional harmonics (*RAE, 2013*). The network connection to the Scottish system, however, is made through overhead AC links and is therefore susceptible to GIC effects (*Erinmez et al., 2002*).

To understand the specific impacts on UK power grid infrastructure, detailed system models are required which include the following aspects: asset location, line orientation and impedance, and transformer grounding type.

4.3 Example of GIC estimates for the UK and impacts on transformers

4.3.1 Estimated GIC for a Carrington-type event

Various scenarios may be used to simulate an extreme GIC event such as:

- Simulating the auroral electrojet current and then the rate of change of the magnetic field. This requires assumptions of the width of the current in the ionophere and its waveform in order to match a Carrington-type event (*Erinmez, 2002*).
- Using historical observations such as magnetic field data recorded by magnetometers during intense geomagnetic storms. The final GIC results are re-scaled to estimate the GIC during a Carrington-type event using a multiplicative factor that is based on the ratio of the peak *Dst* index during a Carrington-type event and the peak *Dst* of the selected event (*Kelly et al., 2017*).
- It is possible to construct a Carrington-type event magnetic field time series for the selected latitude based on the record of the historical event (recorded close to Mumbai in 1859) (*Winter et al., 2017*).

Once the magnetic field has been estimated across the region of interest depending upon the scenario selected, the surface geoelectrical field and finally the GIC across the network can be simulated.

Based on the work of *Winter et al. (2017)*, it has been possible to give a rough estimate of expected GIC considering a simplified transmission line. More accurate analysis requires specific knowledge of UK power grid systems and parameters. Indeed, the specific susceptibility of a given asset is highly dependent on transformer configuration, grounding type, and the existence of protective devices. If a long conductor were present in an electric field that was oriented exactly parallel to the line, the electric field had the intensity of a Carrington-type event, and the resistivity of that line were the same as the default value used in PowerWorld (*PowerWorld, 2018*), we would expect an induced current of 100 to 300 amperes (A). PowerWorld is power system modelling software used in the US, that includes a GIC module for estimating induced currents under given geophysical conditions. These are very rough estimates, and should not be used for planning with specific application to a power grid system model. However, it is consistent with the more detailed analysis performed by *Beggan et al. (2013)*. Their application of a large space weather event to a model of the UK power system compared

the results with data measured at various nodes across the UK. They note the 10 nodes across the UK which experienced the largest GICs during their 200-year return period event, and estimated that the induced currents in these nodes ranged from 131 A to 384 A. *Kelly et al. (2017)* estimated the GIC peak observed at any point in the network in the UK of 290 A for a Carrington-type event, based on the scaled March 1989 event.

4.3.2 Expected GIC impacts

Transformer damage associated with GICs (leading to power disruptions) is often caused by overheating that burns and melts the copper windings and leads of the transformer. The currents that are induced by geomagnetic storms are quasi-DC perturbations to the AC current of the transformer and magnetise the transformer core in one polarity, which can lead to saturation. In this infrequent, high-impact scenario, saturation forces the magnetic flux to escape the core and overheat the transformer. Damage caused by this type of extreme event cannot be repaired, meaning that replacement of the transformer is necessary, which can take months to complete. Some cores are more susceptible to GIC-associated damage than others, as three-phase with five-limb and single-phase cores permit the quasi-DC flux to go directly to the core, while three-phase with three-limb cores have been implemented more recently as they are less prone to this kind of damage (*NRC, 2008*; *RAE, 2013*). Another possible consequence of GICs in the power grid is non-sinusoidal currents, whose harmonics can lead to voltage instabilities. NGC recorded these types of added harmonics in the storms of July 1982, March and October 1989, and November 1991.

The extent to which a network is at risk of GIC damage is dependent on several factors. The higher the voltage in the system, the higher the risk of GIC damage within it. Newer networks, for efficiency reasons, work at higher voltages, and suffer an increased potential for blackouts. This relationship (GIC risk as a function of potential) was found to be nonlinear for a small, 1 V/km induced electric field along a 100 km transmission line (*Radasky, 2011*). Measured GIC is also dependent on the resistance of the transmission lines and surrounding Earth (*RAE, 2013*). Another risk dependency is reactive power demand, which is linear with respect to GIC, but not with respect to voltage of the transformer — i.e., higher voltage requires more reactive power in a nonlinear fashion (*Radasky, 2011*). Reactive power is necessary for voltage control, and the UK grid is now more dependent on reactive compensation equipment, and thus more at risk to GIC damage. Overconsumption of reactive power is a more frequent but less serious GIC-related issue than overheating because there is less potential for transformer damage, but blackouts are still possible (*RAE, 2013*).

4.4 Mitigation strategy

Various measures may be implemented to mitigate a GIC event. These consist of:

- Suitable transformer specification requirements with respect to GIC. For example, a system could be designed to withstand a 120 A neutral current for single-phase transformers in transformer neutrals, and a 300 A (or 100 A per phase) for three-phase transformers. The amperage and the duration for which the transformer must withstand could be estimated from GIC simulation (*Section 4.2*). GIC blocking devices, such as series capacitors, compensation of transmission lines or impedance grounding through resistors, could also be employed.
- Real-time monitoring tools that enable the condition of the transformers or batteries to be assessed by measuring GIC or other system parameters.
- Increasing the number of spare transformers.
- Operating procedures — for example, procedures to prevent overheating or loss of cooling conditions. At a larger scale, measures can be taken to decrease GIC propagation along transmission lines. For example, the following could be increased: the connectivity of the network; the redundancy of transformers at substations; reserves (amount of generation on line).

National Grid mitigation includes forecasting and engineering procedures as mentioned above. Hence, the UK power transmission system is more resilient to geomagnetic disturbances than those in other countries. However, voltage instability could still occur and lead to local blackouts of a few hours and research is still needed to understand the impacts of GIC on transformers (thermal effects, reactive power effect, production of harmonics). Finally, mitigation of this hazard requires collaboration between stakeholders and rapid decision-making in case of a GIC risk (*RAE, 2103*).

In the US, the standard NERC TPL-007-1 (*NERC, 2014*) has recently been established to protect the electric system from the impacts of severe geomagnetic disturbances. Utilities are required to conduct assessments of the impacts of a 1-in-100 year benchmark geomagnetic disturbance event on their equipment and the power system. These include a GIC disturbance vulnerability assessment for the system's ability to withstand a benchmark GMD event without causing a wide area blackout, voltage collapse, or transformer damage, and a transformer thermal impact assessment to ensure that transformers (>200 kV) can withstand thermal transient effects associated with a benchmark GMD event.

4.5 Summary: probability of extreme space weather events and GIC methodology

Assessing the likelihood of extreme space weather events is vital for mitigating future potential risk. Statistical estimates of their annual exceedance probabilities have been carried out; the return period of a Carrington-type event is contained in a rough range of 80 to 500 years. Further studies are needed to refine the estimate and to assess the local variability of the likelihood of these events.

The simulation of GICs requires several inputs: the measurement of the magnetic field at ground level, the ground conductivity model, and technical details of the UK power grid and system assets. GIC intensities are usually modelled at a node of a network (station scale) but fine-scale analysis may be carried out at the transformer level. GIC can seriously damage a transformer. GIC enters the transformer through neutral wires which lead to saturation of the transformer core; harmonics may also be generated in the power system. Saturation and harmonics may lead to heating of transformer cores, burning of windings and malfunction of protective devices. Mitigation strategies must be adopted, and are likely to consist of adequate transformer specifications and operating procedures.

The previous sections focused on the characterisation of extreme geomagnetic storms and GICs. Other processes related to space weather may have a significant impact on UK infrastructure, such as radiation storms (SEPs) and *ionospheric scintillations*.

5.1 Solar energetic particles and *ground level enhancement*

SEP events are characterised as bursts of charged particles (atomic nuclei ranging from hydrogen to uranium) with energies in the order of 10 mega-electronvolts (MeV) to giga-electronvolts (GeV). The largest SEPs occur when several flares and CMEs are ejected within a time span of up to a few days (*Reames, 2013*). The SEPs can travel at up to 80% of the speed of light; thus, their travel time to Earth is much quicker than for CMEs (which generally take a few hours). SEPs affect satellites primarily by causing *single event upsets* (SEUs) in electronic components, which can temporarily disrupt satellite operations (*Lloyd's 360 Risk Insight, 2011*). They also pose a radiation risk to astronauts and airline personnel and passengers on trans-polar flights. For particularly large events, called ground level enhancement (GLE), SEPs may cause upsets in ground electronic systems. Finally, SEPs are associated with *polar cap absorption* (PCA) events which disrupt high frequency radio communications that are frequently used by emergency response personnel (*Kavanagh et al., 2004*). While SEPs are not directly associated with GICs or GIC-related power grid outages, SEP events can occur concurrently with GIC, producing magnetic storms which can affect ground electronics. Due to the associated large PCA events that can encompass the entire British Isles, SEPs must be considered in any comprehensive analysis of space weather risks and impacts on the region.

5.2 Ionospheric scintillation effects on satellite communication and GNSS signal

While there is some degree of randomness (but definite solar cycle dependence for moderate events) in CME, solar flare, and SEP event occurrence, the presence of phenomena such as the solar wind and resulting auroral electrojet are constant. A similar concept applies to the ionosphere, which exists because atmospheric molecules are ionised by EUV radiation that is constantly (and X-ray emission that is less consistently) being emitted by the Sun. The ionosphere is thus always present and indeed is exploited for radio frequency (RF) transmissions. Elevated solar activity at various wavelengths can affect the propagation of these RF signals that are used for communication, navigation and surveillance. In particular, Global Navigation Satellite Systems (GNSS) such as Global Positioning Systems (GPS), Galileo, and Global Navigation Satellite System (GLONASS), can be affected.

The term scintillation refers to random fluctuations in the phase and amplitude of an electromagnetic wave in response to a varying refractive index of the medium in which the

wave is propagating. Scintillation of RF signals is caused by ionospheric plasma density fluctuations and can lead to degradation of the RF signal integrity. This ionospheric scintillation tends to occur most frequently in the equatorial and polar regions of the Earth (SPOSCINDA Report, *AER, 2013*). Systems have been constructed to detect, specify and forecast equatorial *ionospheric scintillation* effects on ultra-high frequency (UHF) and GPS frequencies, which are at ~244 megahertz (MHz) and ~1575 MHz respectively (*Groves et al., 1997*; *Caton et al., 2004*; SPOSCINDA Report, *AER, 2013*). The systems utilise geostationary and GPS satellites that are deployed for military and commercial use.

Note that terrestrial commercial communication systems in the UK are resilient since they are not reliant on GPS. However, *solar radio bursts* can disturb the signals, but only for parts of the network facing the Sun at dawn and dusk (*RAE, 2013*).

5.3 GIC and pipelines

Geomagnetically induced currents are of interest to the oil and gas industries because of the possibility of pipelines being corroded due to geomagnetic storms. The pipes that transport oil and natural gas are usually composed of durable steel insulated with a resistive coating such as paint. Coatings do not necessarily completely insulate the pipes from GICs, as there can be tiny (undetectable) holes in them due to degradation over time or faulty installation. It is this exposure to the surrounding soil and possible currents that leads to corrosion of the pipelines (*Fernberg, 2011*).

Corrosion is defined as the exchange of electrons from one chemical compound to another (i.e. an oxidation-reduction reaction) where charge is preserved. Both oxidation (removal of electrons) and reduction (absorption of electrons) must occur (*Fernberg, 2011*); an example is rust. Steel is the chosen material for the pipelines so that they can endure the pressure associated with copious amounts of oil and natural gas transfer, but when corrosion occurs the material can succumb to the pressure and collapse.

The pipeline and surrounding soil act as an anode-cathode system through which direct ionic current flows, facilitating the oxidation-reduction reaction process. By forcing the direct current to flow only through the pipe (and not through the soil), the entire pipeline can be converted to a cathode, reducing the rate of corrosion. One method of achieving this cathodic protection (CP) system is by connecting the pipeline to a separate anode in the soil (sacrificial CP), thereby deferring the corrosion to another source. Another method is to apply a direct current to maintain a negative voltage in some range to act as a pseudo-reduction reaction to counteract oxidation

(impressed CP). *Pipe-to-soil potential* (PSP) typically should be maintained at a voltage between –1.35 V and –0.85 V to prevent corrosion and disbonding of the coating, but GICs can force the voltage beyond this safe zone, accelerating the corrosion process (*Fernberg, 2011*).

Many observational and theoretical studies, in addition to *Fernberg (2011)*, have been undertaken to investigate the phenomenon of corrosion due to GICs. *Campbell (1978)* and *Campbell (1980)* both analysed magnetometer data measured at sites adjacent to the Alaska oil pipeline. They found a linear relationship between the A_p geomagnetic activity index (daily geomagnetic index derived from the K_p index) and induced current, and that approximately half of the induced currents in the pipeline were less than 1 ampere and thus of little consequence to corrosion, even in pipes not protected with the aforementioned sacrificial CP (though they warn that larger surges in the order of hundreds of amperes are possible and of greater interest). In Finland (70° to 88° latitude), gradients of magnetometers deployed around its pipeline were utilised along with a model based on distributed-source transmission line (*DSTL*) theory to calculate induced electric fields and currents. These model currents agreed reasonably well with the recorded data during one storm that was strong enough to induce a noticeable current in the pipeline. This suggests that a combination of the model and the historical magnetometer data can conceivably be used for a statistical analysis that computes the probability of GIC occurrence (*Pirjola et al., 1999*).

5.4 Hazard combinations

Natural hazards do not often occur in isolation but rather conjointly; for instance, intense wind and rain can create larger impacts than if the hazards occurred individually. Volume 12 — Hazard Combinations describes plausible combinations and includes the space weather hazard. Although the occurrence of a space weather event is independent of the climatic conditions on Earth, some studies have mentioned that lightning activity is modulated by the solar wind and polarity of the Sun's magnetic field (*Scott et al., 2014*; *Owens et al., 2014*).

6. Regulation

Space weather has been included on the National Risk Register of Civil Emergencies since 2011. This UK governmental document summarises the risk of major emergencies that could affect the UK in the next five years. The UK Department for Business, Innovation and Skills published the Space Weather Preparedness Strategy in 2015 (*BEIS, 2015*). This document gathers the progress on built-in resilience to space weather since the risk was added into the National Risk Assessment. There is no specific regulation related to the mitigation of space weather events in the UK. In the US, the Federal North American Electric Reliability Corporation (NERC) adopted a standard NERC TPL-007-1 (*NERC, 2014*) to mitigate the impact of geomagnetic disturbances (GMDs). Coordinators and operators that include transformers with a terminal voltage of more than 200 kV must:

- develop, maintain and implement a GMD operating plan that coordinates the GMD operating procedures or processes within the reliability coordinator area;
- disseminate space weather information;
- develop operating procedures or processes to address a GMD event.

Although such a standard at the UK and EU level does not currently exist, evolution in the regulation over the coming years is expected.

Space weather describes the physical processes of the changing environment between the Sun and the near-Earth space. The dynamical solar magnetic activity is the originator of the space weather that causes sporadic ejections of charged particles that impact the extra-terrestrial environment.

Severe space weather can impact ground-based infrastructure. On the one hand, it changes electric current in space and in the atmosphere, causing rapid geomagnetic field variation on the ground and induced currents. Geomagnetically induced currents flow from the ground to the conductive network, such as transmission lines. GIC may impact the operation of transformers. On the other hand, SEPs may be produced during space weather events, generating secondary particles such as neutrons in the atmosphere. For extreme events, called ground level enhancement (GLE), SEPs may cause upsets in ground electronic systems. Radio and satellite communications (including GNSS signals) may also be disturbed due to fluctuation density of the ionosphere.

The mitigation of space weather events requires (*BEIS, 2015*):

Forecasting

Space weather forecasts analyse the spatial environment from the Sun to the Earth, using satellite and ground sensor observations as well as simulation models. CMEs are assessed as they are the main driver for disruptions in the UK. Some may be directed towards the Earth; their propagation time from Earth to Sun is between 1 and 3 days. Faster ejections lead to greater consequences on Earth. The Carrington-type event travelled to Earth in around 18 hours. However, the orientation and intensity of the magnetic field contained by the CME is essential to assess correctly the impact on Earth. The magnetic orientation of a CME can only be measured when it passes by satellites close to the Earth (in the Sun-Earth line, such as ACE), giving only a 15 to 30 minute warning before it reaches the Earth. Finally, concerning SEP and GLE, energetic particles propagate in about 8 to 10 minutes from the Sun to the Earth atmosphere and are detected by neutron monitors at ground level. Forecasting of such events is impossible; only warnings of a neutron irradiation increase at ground level would be available.

Monitoring

There is no radiation monitor at ground level in the UK; the nearest is in Belgium. As a GLE event can be localised, it is possible that a monitor located outside of the UK may not record an event affecting the UK. Regarding GIC monitoring, the British Geological Survey operates magnetic observatories in the UK that are required to simulate GIC. However, GIC records that are necessary to benchmarks these simulations are very limited.

Reducing system vulnerabilities

In the worst-case scenario, disruption of electrical and electronic devices could occur, power outages, or high frequency telecommunication and GNSS disruptions. Some UK systems are already robust to space weather, compared to other countries. For example, National Grid recently installed transformers with a more resilient design against GIC; and moreover the UK network is highly meshed and possesses shared transformers. UK mobile communication does not rely on GNSS and so will continue to function if the signal is lost. The design of new energy infrastructure could include adequate GIC requirements that will depend on the location of the asset. Voltage instability could still occur and lead to local blackouts of a few hours.

Research is needed to develop GIC forecast models. Nowcast/forecast models of GIC or magnetic field variation on the ground have not yet been tested. The understanding of ionosphere and magnetosphere variations is limited, as is the connection between the different processes taking place between the interplanetary medium, the near-Earth environment and on the ground. Impacts from GLE have been poorly studied and there is no radiation sensor capability in the UK, making it difficult to develop an alert system. However, there are currently UK Natural Environment Research Council funded projects trying to tackle these challenges, such as NERC projects NE/P017231/1 — Space Weather Impacts on Ground-based Systems and NE/R008930/1 — Single Event Effects in Ground Level Infrastructure.

Ádám A, Prácser E, Wesztergom V. 2012. Estimation of the electric resistivity distribution (EURHOM) in the European lithosphere in the frame of the EURISGIC WP2 project. *Acta Geodaetica et Geophysica Hungarica,* 377–387. doi: 10.1556/AGeod.47.2012.4.1

AER. 2013. *SPOSCINDA Analysis Results and Software Production.* Internal AER Report submitted to the Air Force Research Laboratory.

Allen J, Sauer H, Frank L, Reiff P. 1989. Effects of the March 1989 solar activity. *Eos Transactions,* 70, 46. doi: 10.1029/89EO00409

Amm O. 1997. Ionospheric elementary current systems in spherical coordinates and their application. *Journal of Geomagnetism and Geoelectricity,* 49, 947–955. doi: 10.5636/jgg.49.947

Aschwanden MJ. 2005. *Physics of the Solar Corona. An Introduction with Problems and Solutions* (2nd edition). Praxis Publishing Ltd, UK.

Baker DN, Li X, Pulkkinen A, Ngwira CM, Mays ML, Galvin AB and Simunac KDC. 2013. A major solar eruptive event in July 2012: Defining extreme space weather scenarios. *Space Weather,* 11(10): 585–591.

Baumjohann W, Treumann RA. 2004. *Basic Space Plasma Physics.* Imperial College Press, London, UK.

Beggan CD, Beamish D, Richards A, Kelly GS, Thomson AWP. 2013. Prediction of extreme geomagnetically induced currents in the UK high-voltage network. *Space Weather,* 11, 407–419. doi: 10.1002/swe.20065

Beggan CD. 2015. Sensitivity of geomagnetically induced currents to varying auroral electrojet and conductivity models. *Earth, Planets and Space,* 67, 24. doi: 10.1186/s40623-014-0168-9

BEIS. 2015. Space Weather Preparedness Strategy, Version 2.1. https://www.gov.uk/government/publications/space-weather-preparedness-strategy (accessed on 12th July 2018).

Boteler D. 2014. Methodology for simulation of geomagnetically induced currents in power systems. *Journal of Space Weather and Space Climate,* 4, A21. *doi: 10.1051/swsc/2014018*

Campbell WH. 1978. Induction of auroral zone electric currents within the Alaska pipeline. *Pure and Applied Geophysics,* 116, 1143–1173. *doi: 10.1007/BF00874677*

Campbell WH. 1980. Observation of electric currents in the Alaska oil pipeline resulting from auroral electrojet current sources. *Geophysical Journal,* 61, 437–449. *doi: 10.1111/j.1365-246X.1980.tb04325.x*

Caton RG, McNeil WJ, Groves KM, Basu S. 2004. GPS proxy model for real-time UHF satellite communications scintillation maps from the Scintillation Network Decision Aid (SCINDA). *Radio Science,* 39, RS1S22. *doi: 10.1029/2002RS002821*

Cliver EW, Dietrich WF. 2013. The 1859 space weather event revisited: limits of extreme activity. *Journal of Space Weather and Space Climate,* 3. *doi: 10.1051/swsc/2013053*

Denton MH, Borovsky JE, Skoug RM, Thomsen MF, Lavraud B, Henderson MG, McPherron RL, Zhang JC and Liemohn MW. 2006. Geomagnetic storms driven by ICME-and CIR-dominated solar wind. *Journal of Geophysical Research: Space Physics,* 111(A7).

Dungey JW. 1961. Interplanetary magnetic field and the auroral zones. *Physical Review Letters,* 6, 47. *doi: 10.1103/PhysRevLett.6.47*

Eddy JA. 2009. *Sun, the Earth, and Near-Earth Space: A Guide to the Sun-Earth System.* NASA, Washington, DC, USA.

Erinmez IA, Kappenman JG, Radasky WA. 2002. Management of the geomagnetically induced current risks on the National Grid Company's electric power transmission system. *Journal of Atmospheric and Solar-Terrestrial Physics,* 64, 743–756. *doi: 10.1016/S1364-6826(02)00036-6*

ESA. 2018. Solar Weather Expert Service Centre. *http://swe.ssa.esa.int/web/guest/solar-weather* (accessed on 12th July 2018).

Fernberg PA. 2011. *Earth Resistivity Structures and their Effects on Geomagnetic Induction in Pipelines.* PhD thesis, Carleton University, Canada.

Goldstein J. 2006. Plasmasphere response: tutorial and review of recent imaging results. *Space Science Reviews,* 124, 203–216. *doi: 10.1007/s11214-006-9105-y*

Gosling JT, Bame D, McComas J, Phillips L. 1990. Coronal mass ejections and large geomagnetic storms. *Geophysical Research Letters,* 17, 7, 901–904. *doi: 10.1029/GL017i007p00901*

Groves KMS, Basu EJ, Weber EJ, Smitham M, Kuenzler H, Valladares CE, Sheehan R, MacKenzie E, Secan JE, Ning P, McNeill WJ, Moonan DW, Kendra MJ. 1997. Equatorial scintillation and systems support. *Radio Science,* 32, 2047–2064. *doi: 10.1029/97RS00836*

Kappenman JG. 2005. An overview of the impulsive geomagnetic field disturbances and power grid impacts associated with the violent Sun-Earth connection events of 29–31 October 2003 and a comparative evaluation with other contemporary storms. *Space Weather,* 3, S08C01. *doi: 10.1029/2004SW000128*

Kavanagh A, Marple S, Honary F, McCrea I, Senior A. 2004. On solar protons and polar cap absorption: constraints on an empirical relationship. *Annales Geophysicae,* 22, 1133–1147. *doi: 10.5194/angeo-22-1133-2004*

Kelly GS, Viljanen A, Beggan CD, Thomson AWP. 2017. Understanding GIC in the UK and French high-voltage transmission systems during severe magnetic storms. *Space Weather,* 15, 99–114. *doi: 10.1002/2016SW001469*

Lanzerotti LJ. 1992. Comment on 'Great magnetic storms' by Tsurutani et al. *Geophysical Research Letters,* 19, 1991–1992. *doi: 10.1029/92gl02238*

Launay R. 2014. Solar storms and their impacts on power grids: Recommendations for (re) insurers. *https://www.apref.org/sites/default/files/espacedocumentaire/2014_05_20_solar_storms_apref.pdf* (accessed on 12th July 2018).

Li X, Temerin M, Tsurutani BT, Alex S. 2006. Modeling of 1–2 September 1859 super magnetic storm. *Advanced Space Research,* 38, 273–279. *doi: 10.1016/j.asr.2005.06.070*

Lloyd's. 2013. Solar storm risk to the North American electric grid. *https://www.lloyds.com/news-and-insight/risk-insight/library/natural-environment/solar-storm* (accessed on 12th July 2018).

Lloyd's 360 Risk Insight. 2011. *Space Weather: Its impact on Earth and implications for business.* London, UK.

Marusek JA. 2007. Solar storm threat analysis. *Impact.* Available at: *https://www.jumpjet.info/Emergency-Preparedness/Disaster-Mitigation/NBC/EM/Solar_Storm_Threat_Analysis.pdf* (accessed on 12th July 2018).

Met Office. 2015. Space Weather: Measuring the impact. *http://www.metoffice.gov.uk/publicsector/emergencies/space-weather/uk-scales* (accessed on 12th July 2018).

MITRE. 2011. *Impacts of Severe Space Weather on the Electric Grid.* Washington, DC, USA: The Department of Homeland Security. Available at: *https://fas.org/irp/agency/dod/jason/spaceweather.pdf* (accessed on 12th July 2018).

NASA. 2018. Coordinated Data Analysis Web. *https://cdaweb.sci.gsfc.nasa.gov/index.html/* (accessed on 12th July 2018).

NERC. 2014. TPL-007-1: Establish requirements for Transmission system planned performance during geomagnetic disturbance (GMD) events. *https://www.nerc.com/pa/Stand/Pages/TPL0071RI.aspx* (accessed on 12th July 2018).

NRC. 2008. *Severe Space Weather Events — Understanding Societal and Economic Impacts: A Workshop Report.* The National Academies Press, Washington, DC, USA. *doi:10.17226/12507*

Owens MJ, Scott CJ, Lockwood M, Barnard L, Harrison RG, Nicoll K, Watt C, Bennett AJ. 2014. Modulation of UK lightning by heliospheric magnetic field polarity. *Environmental Research Letters,* 9, 115009. *doi: 10.1088/1748-9326/9/11/115009*

Pirjola R, Pulkkinen A, Viljanen A, Nevanlinna H, Pajunpää K. 1999. Study explores space weather risk to natural gas pipeline in Finland. *EOS Transactions,* 80, 332–333. *doi: 10.1029/99EO00249*

PowerWorld. 2018. PowerWorld: The visual approach to electric power systems. *https://www.powerworld.com/* (accessed on 12th July 2018).

Pulkkinen A, Bernabeu E, Eichner J, Beggan C, Thomson AWP. 2012. Generation of 100-year geomagnetically induced current scenarios. *Space Weather,* 10, S04003. *doi: 10.1029/2011SW000750*

Radasky WA. 2011. Overview of the impact of intense geomagnetic storms on the U.S. high voltage power grid. *IEEE International Symposium on Electromagnetic Compatibility,* 300–305. *doi: 10.1109/ISEMC.2011.6038326*

RAE. 2013. *Extreme Space Weather: Impacts on Engineered Systems and Infrastructure.* Royal Academy of Engineering, Prince Philip House, 3 Carlton House Terrace, London, UK. *https://www.raeng.org.uk/spaceweather* (accessed on 12th July 2018).

REAL. 2012. Geoelectric Litosphere Model of the Continental Europe. *http://real.mtak.hu/2957/* (accessed on 12th July 2018).

Reames DV. 2013. The two sources of solar energy particles. *Space Science Reviews,* 175, 53. *doi: 10.1007/s11214-013-9958-9*

Richardson IG, Cane HV. 2013. Near-Earth solar wind flows and geomagnetic activity over more than four solar cycles (1963–2011). AIP Conference Proceedings, 1539, 426 *doi: 10.1063/1.4811076*

Riley P. 2012. On the probability of occurrence of extreme space weather events. *Space Weather,* 10, S02012. *doi: 10.1029/2011SW000734*

Schrijver C, Kauristie K, Aylward AD, Denardini CM, Gibson SE, Glover A, Gopalswamy N, Grande M, Hapgood M, Heynderickx D, Jakowski N, Kalegaev W, Lapenta G, Linker JA, Lui S, Mandrini CH, Mann IR, Nagatsuma T, Nandy D, Obara T , O'Brien P, Onsager T, Opgenoorth HJ, Terkildsen MT, Valladares CE, Vilmer N, COSPAR/ILWS Space Weather Panel 2015. 2015. Understanding space weather to shield society: A global road map for 2015–2025 commissioned by COSPAR and ILWS. *Advances in Space Research,* 55, 2745–2807. *doi: 10.1016/j.asr.2015.03.023*

Schwenn R. 2006. Space weather: the solar perspective. *Living Reviews in Solar Physics,* 3, 2. *doi: 10.12942/lrsp-2006-2*

Scott CJ, Harrison RG, Owens MJ, Lockwood M, Barnard L. 2014. Evidence for solar wind modulation of lightning. *Environmental Research Letters,* 9, 055004. *doi: 10.1088/1748-9326/9/5/055004*

Siscoe G, Crooker NU, Clauer CR. 2006. *Dst* of the Carrington storm of 1859. *Advances in Space Research,* 38, 173–179. *doi: 10.1016/j.asr.2005.02.102*

Stern DP. 1994. The art of mapping the magnetosphere. *Journal of Geophysical Research,* 99, 17169–17198. *doi: 10.1029/94JA01239*

Sugiura M, Kamei T. 1991. *Equatorial Dst index 1957–1986.* Saint-Maur-des-Fosses, France: ISGI Publications Office.

SWPC. 2018a. NOAA Space Weather Prediction Center. *https://www.swpc.noaa.gov* (accessed on 12th July 2018).

SWPC. 2018b. Planetary K-index. *https://www.swpc.noaa.gov/products/planetary-k-index* (accessed on 12th July 2018).

Temerin M, Li X. 2006. *Dst* model for 1995–2002. *Journal of Geophysical Research,* 111, A04221. *doi: 10.1029/2005JA011257*

Thomson AWP, McKay AJ, Clarke E, Reay SJ. 2005. Surface electric fields and geomagnetically induced currents in the Scottish Power grid during the 30 October 2003 geomagnetic storm. *Space Weather,* 3, S11002. *doi: 10.1029/2005SW000156*

Thomson AWP, Dawson EB, Reay SJ. 2011. Quantifying extreme behavior in geomagnetic activity. *Space Weather,* 9, S10001. *doi:10.1029/2011SW000696*

Tripathi R, Mishra AP. 2006. Occurrence of severe geomagnetic storms and their association with solar-interplanetary features. *ILWS Workshop, Goa, February 19–24, 2006.* Available at: *https://cdaw.gsfc.nasa.gov/publications/ilws_goa2006/095_Tripathi.pdf* (accessed on 12th July 2018).

Tsubouchi K, Omura Y. 2007. Long-term occurrence probabilities of intense geomagnetic storm events. *Space Weather,* 51, S12003. *doi: 10.1029/2007SW000329*

Tsurutani BT, Gonzalez WD, Lakhina GS, Alex S. 2003. The extreme magnetic storm of 1–2 September 1859. *Journal of Geophysical Research,* 108, 12–68, SSH 1-1. *doi: 10.1029/2002JA009504*

UMA. 2018. Forecasting Solar Energetic Proton events. *http://spaceweather.uma.es/solarstorms.html* (accessed on 12th July 2018).

Vasseur G, Weidelt P. 1977. Bimodal electromagnetic induction in non-uniform thin sheets with an application to the northern Pyrenean induction anomaly. *Geophysical Journal International,* 51, 669–690. *doi: 10.1111/j.1365-246X.1977.tb04213.x*

Viljanen A, Nevanlinna H, Pajunpää K, Pulkkinen A. 2001. Time derivative of the horizontal geomagnetic field as an activity indicator. *Annales Geophysicae,* 19, 1107–1118.

Viljanen A, Pirjola R, Wik M, Ádám A, Prácser E, Sakharov Y and Katkalov J. 2012. Continental scale modelling of geomagnetically induced currents. *Journal of Space Weather and Space Climate,* 2, A17. *doi: 10.1051/swsc/2012017*

Viljanen A, Pirjola R, Prácser E, Katkalov J, Wik M. 2014. Geomagnetically induced currents in Europe. Modelled occurrence in a continent-wide power grid. *Journal of Space Weather and Space Climate,* 9. *doi: 10.1051/swsc/2014006*

Winter LM, Gannon J, Pernak R, Huston S, Quinn R, Pope E, Ruffenach A, Bernardara P, Crocker N. 2017. Spectral scaling technique to determine extreme Carrington-level geomagnetically induced currents effects. *Space Weather,* 15, 713–725. *doi: 10.1002/2016SW001586*

Yashiro S, Gopalswamy N, Michalek G, St. Cyr OC, Plunkett SP, Rich NB, Howard RA. 2004. A catalog of white light coronal mass ejections observed by the SOHO spacecraft. *Journal of Geophysical Research,* A07105. *doi: 10.1029/2003JA010282*

Astronomical unit (au)

Defined as exactly 149,597,870,700 meters. It is the average distance between the Earth and the Sun.

Aurora

Sporadic radiation emission, appearing as streamers of light, that usually occurs in the northern or southern sky regions of the Earth. It is caused by charged particles that precipitate into the upper atmosphere during periods of Earth's magnetic field disturbances.

Auroral electrojet

A horizontal electric current flowing region of the ionosphere. They form ovals centred around the magnetic poles. Their latitudinal positions and strength are variable and depend on the geomagnetic activity.

Coronal hole

A darker area on the Sun, less dense and cooler than its surrounding region where fast solar winds are produced.

Coronal interaction region (CIR)

Regions localised at the interface between slow and fast solar wind. Intense magnetic fields can be produced in these regions.

Coronal mass ejection (CME)

Generated from the outer solar atmosphere, the corona, that is structured by magnetic fields. Plasma can be confined inside these fields and suddenly be released into the interplanetary medium. Larger CMEs can contain a billion tons of matter with an average speed of 400 km/s. They may be directed into the Earth, impacting the extra-terrestrial environment.

Dayside

The side of the planet facing its star. In the case of the Earth, the side in the Earth-Sun line direction.

Geo-effectiveness

Related to the capacity of physical processes to produce a geomagnetic disturbance.

Ground level enhancement (GLE)

Sudden increases in the count rates of neutrons due to SEP events recorded by ground-based detectors at ground level.

Halo CME

A CME that propagates in a direction close to the Sun-Earth line and is observed by a coronagraph.

Interplanetary magnetic field (IMF)

The magnetic field embedded in the solar wind and dragged into interplanetary space.

Ionospheric scintillation

The rapid modification of radio waves caused by small-scale structures in the ionosphere.

Magnetic reconnection

Related to the breaking and reconnecting of oppositely directed magnetic field lines in a plasma. In the process, magnetic field energy is converted to plasma kinetic and thermal energy.

Magnetosphere

An area of space, around a planet, that is controlled by the planet's magnetic field. It is formed by the interaction of solar wind with the planet's magnetic field.

Magnetotail

An elongated region of the magnetosphere of the Earth or of another planet that extends in the direction away from the Sun.

Nanotesla

The tesla (T) is the derived unit of the magnetic flux density. It is equal to one weber per square meter. 1 nanotesla (nT) = 10^{-9} tesla.

Parker spiral

The rotation of the Sun forces the magnetic field streamlines to form a spiral shape, known as the Parker spiral (or the Archimedean spiral).

Pipe-to-soil potential

Voltage potential generated between a buried pipe and its surrounding soil.

Plasma

A state of matter in which the atoms are ionised.

Polar cap absorption (PCA)

PCA events are related to the increased ionisation due to solar particle events that absorbs radio waves in the high-frequency and very high-frequency bands.

Reactive power

The power required to maintain adequate voltage in the system.

Ring current

One of the current systems in the Earth's magnetosphere. It is carried by charged energetic particles (10 to 200 kilo electronvolt) that are trapped in the magnetosphere and circle the Earth.

Saturation (magnetic)

The maximum capacity of a substance or element to store magnetism. When a transformer is saturated, harmonics on the output voltage of the transformer are created and disturb its electrical system.

Single event upset (SEU)

An unintentional change of state of a silicon device (integrated circuit) that is caused by ionising radiation strikes.

Solar energetic particle (SEP)

A high-energy particle coming from the Sun. It can be a proton, electron or heavy ion with energy ranging from a few tens of mega to giga electronvolt.

Solar flare

An intense burst of radiation (covering a large part of the spectrum) that follows the release of magnetic energy associated with sunspots.

Solar radio burst

This consists of radio waves that cover a broad waveband created by a solar flare.

Solar wind

A continuous flow of protons and electrons produced by the Sun and propagating into interplanetary space. There are two regimes of solar wind: fast and slow. Slow solar wind has a velocity of 300 to 500 km/s, compared to more than 700 km/s for fast solar wind. Fast solar wind originates from coronal holes.

Abbreviations

AC	Alternating current
ACE	Advanced Composition Explorer spacecraft
AE	Auroral electrojet
AEP	Annual exceedance probability
AU	Astronomical Unit
BGS	British Geological Survey
CIR	Coronal interaction region
CME	Coronal mass ejection
CP	Cathodic protection
DC	Direct current
Dst	Disturbance storm time
DSTL	Distributed-source transmission line
ESA	European Space Agency
EURISGIC	European Risk for Geomagnetically Induced Currents
EUV	Extreme ultraviolet
FERC	Federal Energy Regulatory Commission
GIC	Geomagnetically induced current
GLE	Ground level enhancement
GLONASS	Global Navigation Satellite System
GMD	Geomagnetic disturbance
GNSS	Global Navigation Satellite Systems
GOES	Geostationary Operational Environmental Satellites
GPS	Global Positioning System
IMF	Interplanetary magnetic field
MOSWOC	Met Office Space Weather Operations Centre
NASA	National Aeronautics and Space Administration
NERC	North American Electric Reliability Corporation
NGC	National Grid Company
NOAA	National Oceanic and Atmospheric Administration
PCA	Polar cap absorption
PSP	Pipe-to-soil potential
RAE	Royal Academy of Engineering
RF	Radio frequency
SEP	Solar energetic particle

Abbreviations

SEU	Single event upset
SOHO	Solar and Heliospheric Observatory
SPOSCINDA	Space Programs Office Scintillation Network Decision Aid
SWPC	Space Weather Prediction Centre
UHF	Ultra-high frequency

LC 0064_18V10

EDF ENERGY

energy technologies institute

IChemE ADVANCING CHEMICAL ENGINEERING WORLDWIDE

Institution of MECHANICAL ENGINEERS

Met Office

MOTT MACDONALD